

Time-resolved circularly polarized luminescence of Eu³⁺-based systems

Uri Hananel¹ | Gal Schwartz¹ | Guy Paiss¹ | Lorenzo Arrico² |
 Francesco Zinna² | Lorenzo Di Bari² | Ori Cheshnovsky¹ | Gil Markovich¹

¹School of Chemistry, Tel Aviv University, Tel Aviv, Israel

²Department of Chemistry and Industrial Chemistry, University of Pisa, Pisa, Italy

Correspondence

Gil Markovich, School of Chemistry, Tel Aviv University, Tel Aviv 6997801, Israel.
 Email: gilmar@post.tau.ac.il

Funding information

Israel Science Foundation, Grant/Award Number: 338/18

Abstract

Chiral Eu³⁺-based systems are frequently studied via circularly polarized luminescence spectroscopy. The emission lifetimes of each circular polarization, however, are virtually always ignored, because in a homogeneous sample of emitters, there should be no difference between the two. However, we show that in less robust Eu³⁺ complex structures, as in the chiral complex Eu (facam)₃, a difference in the lifetimes of the two circularly polarized emission components arises due to heterogeneity of the complexes. In this case, each species within the sample could have different degrees of circularly polarized luminescence and decay rates at certain emission lines. The superposition of the emission components of the various chiral species leads to an overall difference in decay rate between the two circular polarizations. Such a difference is also shown for Eu³⁺-doped chiral TbPO₄·D₂O nanocrystals. We believe that this kind of measurement could be a unique tool for determining the homogeneity of a lanthanide-based chiral system, where other methods might fail in this task.

KEY WORDS

chiral complexes, chiral nanocrystals, emission lifetime, lanthanide complexes

1 | INTRODUCTION

Circularly polarized luminescence spectroscopy is based on the unequal emission of right and left circularly polarized light (R- and L-CPL, respectively) by chiral species.¹ This is interpreted as different transition probabilities for the emission of the two circular polarizations. Traditionally, the measured quantity is the emission circular intensity difference (ECID), $I_L - I_R$, where I_L and I_R are the L- and R-CPL steady-state emission intensities (measured under continuous excitation), respectively. ECID is related to the luminescence dissymmetry factor, $g_{lum} = 2(I_L - I_R)/(I_L + I_R)$, which is on the order of 10^{-3} or less for most (luminescent) organic chiral molecules and

significantly higher for some emission lines of chiral lanthanide complexes and supramolecular assemblies.² Although there are some chiral organic architectures with higher g_{lum} , they are rare and still fall short of chiral lanthanide complexes.^{3,4}

Chiral europium(III) complexes are well known for their emission lines with strong g_{lum} . Their photophysical properties are relatively simple compared with other lanthanides, as the emitting level, labeled 5D_0 , is non-degenerate, and a set of transitions from this level to the manifold of the 7F_J ($J = 0-6$) states can be typically observed. For example, the $^5D_0 \rightarrow ^7F_1$ transition would typically have a strong ECID, being magnetic dipole allowed and electric dipole forbidden. Hence, the emission rates of L- and R-CPL for this line should be significantly different. Nevertheless, because there is a single

Uri Hananel and Gal Schwartz contributed equally to this work.

emitting level, the lifetimes of the two circular polarizations should be identical. This is because the emission decay rate is proportional to the excited-state population, $N(t)$, which is depleted in parallel by the two emitted circular polarization channels:

$$\frac{dN(t)}{dt} = (A_L + A_R + A_{NR})N(t)$$

where A_L, A_R are the transition rate coefficients of the two circular polarizations and A_{NR} is the non-radiative decay rate.

Because the emission intensity $I(t) \propto N(t)$ and

$$N(t) = N_0 e^{-At}$$

where $A = A_L + A_R + A_{NR}$, then the two circularly polarized emission components should decay with the same time constant: $\tau = 1/A$.

This statement is true given a homogeneous sample of a chiral Eu^{3+} compound, or for that matter any sample with a single emitting excited state. It might not be the case in other lanthanides, where there is a multiplicity of emitting excited-state levels. Each of these excited states might have different coefficients for the emission rates of the two circular polarizations and possibly also different lifetimes. Alternatively, one could expect different lifetimes for the two circular polarizations when there is a nonhomogeneous distribution of the chiral Eu^{3+} species, with each subpopulation having its own specific ECID magnitude, sign, and lifetime.

In general, time-resolved circularly polarized luminescence (TR-CPL) was found useful in cases where either the emitter undergoes changes in its emitting levels on a timescale of the decay process or the emitting sample itself is heterogeneous, with different components exhibiting different lifetimes. The former was observed for protein dynamics and the latter for enantiospecific interactions between a chiral emitter and a racemic non-emitting species.^{5–8} Recently, a novel TR-CPL setup was used to isolate long-lived CPL emission from a sample also containing shorter-lived emitters which do not contribute to the CPL.⁹ Yet, TR-CPL was not used to probe a sample of a (supposedly) single chiral species and thus infer on its homogeneity.

The purpose of this publication is to show that the difference in circularly polarized emission lifetimes can be used to deduce on the existence of inhomogeneity in the lanthanide ion sites, which might be difficult to detect using other techniques. In this work, we examined several chiral Eu^{3+} compounds, looking for TR-CPL, measured as a difference in the decay rates between the two emitted circular polarizations, in samples which supposedly contain

a single emitting species. In order to explore different Eu^{3+} -based chiral systems with fairly high g_{lum} values for the possible appearance of emitted circular polarization lifetime differences, we chose to study four different types of samples: Two well-known Eu^{3+} -based fluoro-camphorate-type chiral complexes, which we expected to have different levels of conformational robustness, and two very different types of crystalline solids (polycrystalline solid chiral complex and colloidal chiral inorganic nanocrystals [NCs]) samples, where more complex excitation dynamics may occur. In particular, we found such a difference in the commercially available enantiomerically pure (+)- $\text{Eu}(\text{facam})_3$ complex ($\text{facam} = 3\text{-}(3\text{-trifluoromethylhydroxymethylene})\text{-}(+)\text{-camphorate}$), a common ECID calibration standard. We also found such a difference in a markedly different system, Eu^{3+} -doped chiral NCs.

2 | MATERIALS AND METHODS

2.1 | Sample preparation

2.1.1 | (+)- $\text{Eu}(\text{facam})_3$

Europium tris[3-(trifluoromethylhydroxymethylene)-(+) -camphorate], anhydrous dimethyl sulfoxide (DMSO) (99.9%), and molecular sieves 3 Å were purchased from Sigma and stored in a nitrogen glovebox.

2.1.2 | (+)- $\text{Eu}(\text{facam})_3$ solution

Activated molecular sieves were added to the solvent, and the complex was dissolved in dry DMSO to the desired concentration. The sample was freshly prepared before each measurement under nitrogen in a glovebox.

2.1.3 | (+)- $\text{Eu}(\text{facam})_3$ solid

A microscope glass slide was thoroughly washed with ethanol and isopropanol and then dried under N_2 . Several μL of a 50-mM (+)- $\text{Eu}(\text{facam})_3$ solution in dry DMSO were drop-cast on the slide, which was then dried under low vacuum overnight.

2.1.4 | (+/-)- CsEu(hfbc)_4

The complex ($\text{hfbc} = 3\text{-heptafluorobutylrylcamphorate}$) was synthesized according to the protocol of ref. 10. The obtained solid was dissolved in dry acetonitrile to a 4-mM solution prior to its measurement.

2.2 | Eu³⁺-doped TbPO₄·D₂O NCs

The NCs were synthesized according to the protocol of ref. 11. After purification of the produced NCs by centrifugation, the same volume of solvent (D₂O) was used to re-disperse them.

2.3 | Circularly polarized luminescence measurements

All steady-state ECID measurements were performed using a homebuilt photoelastic modulator-based CPL spectrometer described in ref. 12 (see Figure 1a). The samples were excited using 395 (Vortran Stradus 395-100), 405 (Toptica iBeam smart 405 nm 100 mW), and 488 (Techhood 488 nm 60 mW) nm diode lasers with excitation and emission edgepass filters. A shortpass filter

with a cutoff wavelength of 450 nm was used for the 395- and 405-nm lasers, and a similar one with cutoff wavelength of 500 nm was used for the 488-nm laser. The emission longpass filter had a cutoff wavelength of 550 nm. For all solution-based measurements, a Thorlabs fused silica cuvette of 1-cm optical path length was used.

TR-CPL measurements (Figure 1b) were performed with the same homebuilt CPL apparatus, except:

(i) Instead of continuous excitation, the samples were excited with a laser diode modulated by a square-wave trigger with a duty cycle of 20% and 100-Hz frequency. The emission intensity sampling rate was 100 kHz. The fall time of the laser pulse was <10 µs, and emission signal acquisition was started 30 µs after the laser trigger turnoff.

(ii) Instead of a photoelastic modulator, the individual L- or R-CPL components of the emission were measured via a Thorlabs AQWP05M-600 achromatic λ/4 waveplate,

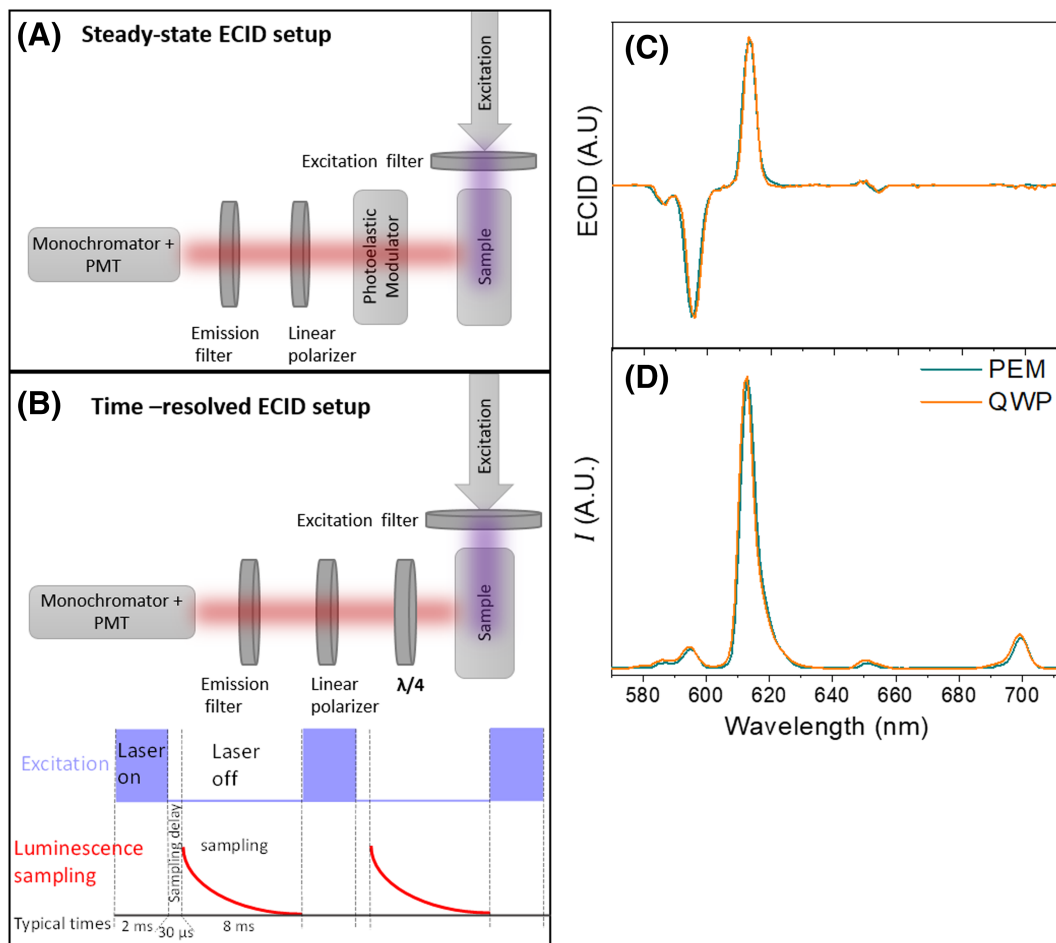


FIGURE 1 The two configurations used for the measurements performed in this work and comparison of their performance. (a) The photoelastic modulator-based setup for steady-state measurement of ECID. (b) The setup for circularly polarized emission lifetime measurements of solution-based samples, where each circular polarization's lifetime is measured separately by rotating the λ/4 plate by 90°. At the bottom of this panel, the timing sequence of the TR-CPL measurement is sketched. The ECID (c) and total emission (d) spectra of a model sample Eu (facam)₃ taken in the two setups seem to overlap well

followed by a linear polarizer. The two emitted circular polarizations were measured sequentially by rotating the $\lambda/4$ waveplate $\pm 45^\circ$ with respect to the linear polarizer axis to factor out the polarization transmission dependence of the monochromator.

It should be stressed that the steady-state spectra could also be measured using the TR-CPL setup, as demonstrated in Figure 1c,d. However, because the photoelastic modulator based setup is more sensitive and accurate for ECID measurements, we normally used this setup for the spectral measurements.

An important part of the data analysis was the fitting of the polarized emission decay curves to either single or two exponential functions and estimation of the error in this procedure. More information about the exact fitted expressions and how errors were estimated is provided in the Supporting Information.

3 | RESULTS AND DISCUSSION

In many of the emitting lanthanide-based systems, there is an absorbing donor transferring the excitation energy to the emitting species (Eu^{3+} in the present case). This involves a relatively short rise time of the emission. As we were interested purely in the emitting state lifetime, we ignored this short rise time and very early emission and focused only on the post-peak emission intensity decay (see timing scheme in Figure 1b). This is because the aim in this work is not to measure the lifetime with upmost accuracy, but rather to measure differences between two measured lifetimes of the same emitter with the highest precision. By omitting the sampling of emission rise time and possibly the start of the decay, we avoid errors introduced by data analysis which might arise from deconvoluting the instrumental response function with the emission data. For this purpose, we modulated the excitation laser intensity with a square-wave trigger and started recording the emission intensity decay shortly after the excitation laser shutoff. The on-time of the laser was typically several milliseconds, which was found to be sufficiently long for the sample to reach steady-state emission conditions. This was confirmed in all experiments, where the chosen laser modulation frequency (and duty cycle) was confirmed not to affect the decay curves (see Figure S1).

We examined the emission decay of the two circular polarizations of the chiral complex CsEu(hfbc)_4 in acetonitrile, whose magnitude of ECID activity at the $J = 1$ emission line (595 nm) is $g_{\text{lum}} = -0.98$, comparable with Eu(facam)_3 , at the same line (Figure 2). In this complex, the coordination sphere around the Eu^{3+} emitter is full (eight-dentate), and the structure is further stabilized by

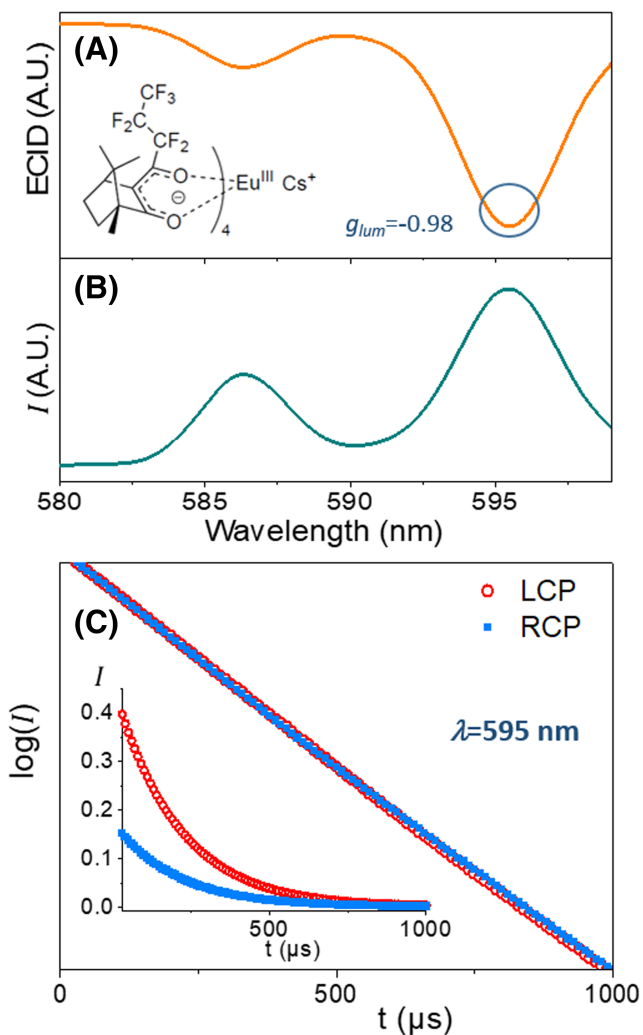


FIGURE 2 (a) ECID and (b) total emission spectra of 4-mM (+)- CsEu(hfbc)_4 complex dissolved in acetonitrile. Peak g_{lum} value is indicated at the arrow. (c) The normalized logarithm of the intensities of the two emitted circular polarizations at 595 nm versus time for the same solution. Excitation wavelength = 405 nm with 25-mW power. Inset: The raw intensities of the two circular polarizations plotted on a linear scale. The data are an average of 50,000 measurement cycles per each emitted circular polarization. The 405-nm photons excite the hfbc ligands, which transfer the excitation energy to the Eu^{3+} ion. The decay curves were fitted with a single exponent and the lifetimes were 201 ± 2 and $203 \pm 1 \mu\text{s}$ for the L- and R-CPL decays, respectively

the cesium ion.¹⁰ There is strong evidence that only a single species of the complex is present in solution.¹³ This makes this complex a good benchmark for how a chiral homogeneous emitting Eu^{3+} sample with high g_{lum} should behave in TR-CPL, namely, it should not display any difference between the decay rates of the two polarizations. Hence, these results can serve as a baseline experiment to characterize the threshold level in determining whether such a difference can be observed in our measurement setup.

Figure 2 shows the normalized logarithm of the two emitted circular polarization intensities at 595 nm as a function of time. The normalized logarithm of the TR-CPL curves provides an excellent visual evidence of how a zero difference in decay rates appears. Because the logarithm of the emission intensity is nearly a straight line, the decay function is well approximated by a single exponent. From this, we can obtain a numerical value for our uncertainty level by quantifying the difference in lifetimes as $g_{lif} = (\tau_L - \tau_R)/(1/2(\tau_L + \tau_R))$, where τ_L and τ_R are the lifetimes of the L- and R-CPL decays, accordingly. This amounts to $g_{lif} = 0.6 \times 10^{-3}$, and so we use $\sim 1 \times 10^{-2}$ as the uncertainty level in determination of g_{lif} . We note that $g_{lif} \rightarrow 0$ in the limit of a noise-free measurement of a homogeneous emitter.

We next turn our attention to (+)-Eu (facam)₃. Because we only studied this commercially available

enantiomer, we shall refer to it henceforth as simply Eu (facam)₃. We focused on the emission line at 595 nm ($J = 1$), which displays the highest g_{lum} value, -0.78 , and compared it with the emission line at 614 nm ($J = 2$), with an order-of-magnitude lower g_{lum} value, $+0.078$ (see Figure 3). The 595-nm emission line corresponds to a magnetic dipole allowed transition from the ⁵D₀ singlet level to the probably doubly degenerate crystal-field sublevel of the ⁷F₁ state,¹⁴ assuming C₃ symmetry for the complex. It should be stressed that a multiplicity in the lower state should not in itself cause a difference in lifetimes between the two circular polarizations, because they only depend on the upper state population $N(t)$.

Water molecules are known to strongly bind to Eu³⁺ and affect the ECID of Eu (facam)₃.¹⁵ Hence, we took measures to ensure the total dryness of the sample: We stored and prepared samples in a nitrogen-filled glovebox

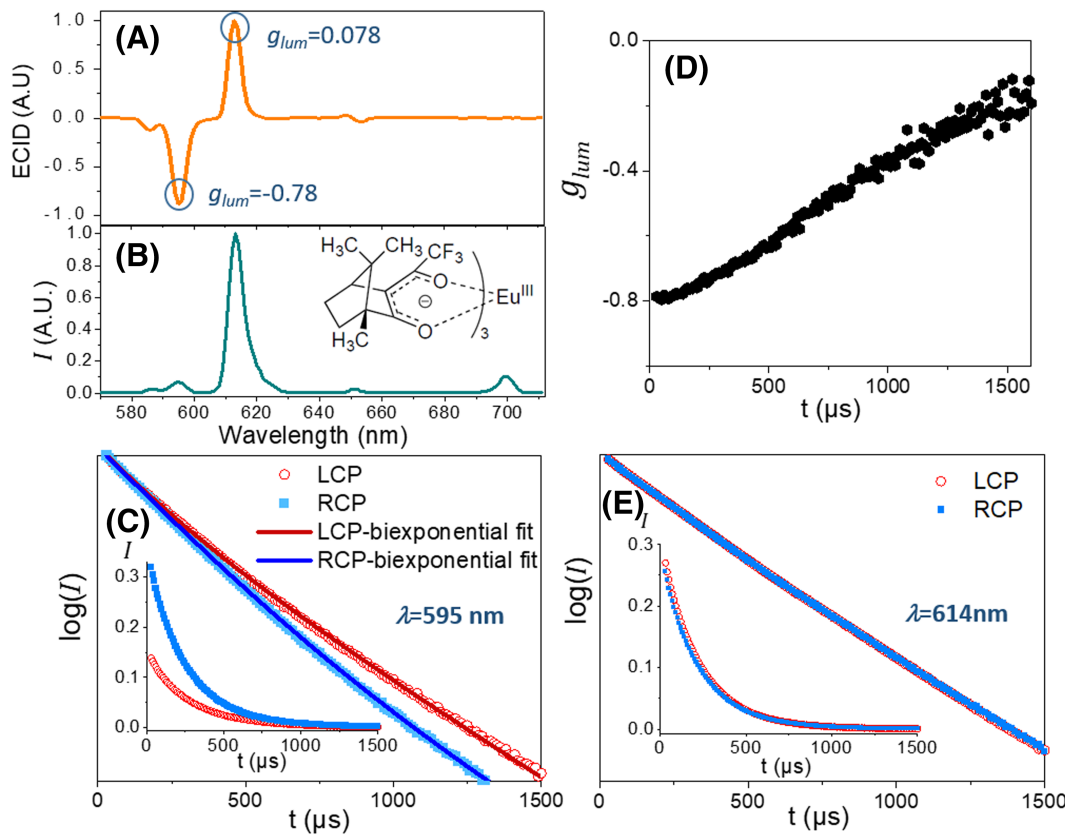


FIGURE 3 (a) ECID and (b) total emission spectra of a 5-mM solution of Eu (facam)₃ in dry DMSO. The total emission, ECID, and decay of L- and R-CPL emission intensity of the same solution were measured using excitation wavelength = 395 nm with 50-mW power. The data are an average of 6000 measurement cycles per each emitted circular polarization. The 395-nm photons directly excite the ⁷F₀ → ⁵L₆ transition of the Eu³⁺ ion¹⁴ and probably the ligands as well. (c) The normalized logarithm of the intensities of the two emitted circular polarizations (at 595 nm). The decay curves were fitted with a sum of two exponents, and the amplitude weighted lifetimes were 281 ± 4 and 252 ± 2 μs for the L- and R-CPL decays, respectively. The inset of (c) is the raw emission intensity decay of the two circular polarizations plotted on a linear scale. (d) The time-dependent dissymmetry factor, $g_{lum}(t)$, measured at 595 nm. (e) The normalized logarithm of the intensities of the two emitted circular polarizations at 614 nm ($g_{lum} = 0.078$). Inset of (e) is the raw emission intensity decay of the two circular polarizations plotted on a linear scale.

using 99.9% DMSO. We also used molecular sieves to ensure complete dryness during the measurement, which took place outside the glovebox.

In Figure 3c, it is clearly seen that the two emitted circular polarizations differ in their decay rates and that they are not monoexponential functions of time. In fact, they can be fitted well with a sum of two exponential functions with the parameters shown in Table 1. We believe that the different decay rates and multi-exponential form of the decay curves reflect sample heterogeneity, as will be discussed later on.

Another way of observing such a difference is through a plot of the time-dependent luminescence dissymmetry factor $g_{\text{lum}}(t) = (I_L(t) - I_R(t))/(1/2(I_L(t) + I_R(t)))$ shown in Figure 3d. It should be emphasized that plotting $g_{\text{lum}}(t)$ is merely a convenient way to represent the difference and trends in the decay curves of the two polarizations and does not bear an important physical significance on its own. As observed in Figure 3d, $g_{\text{lum}}(t)$ starts at ~ -0.8 , at $t \approx 0$, in agreement with the value of the steady-state g_{lum} of the 595-nm line of Eu(facam)₃, -0.78 .¹⁶ A significant change is observed in $g_{\text{lum}}(t)$, decreasing in a roughly linear fashion with time toward zero with a time constant on the order of 1 ms, which is longer than the average emission lifetime. Thus, the plot of $g_{\text{lum}}(t)$ might indicate that the heterogeneity of the emitting species is expressed mostly at the tail of the emission decay. This is very relevant because it may be quite challenging to study different conformations of Eu³⁺ or other lanthanide complexes with common spectroscopic techniques such as NMR when the ligand exchange rates fall in the fast or intermediate NMR timescale regime.¹⁷ Moreover, in the case of Eu³⁺, EPR is precluded as well, as it is EPR inactive (due to its nondegenerate ground level).^{14,18}

The difference in decay rates did not depend on Eu(facam)₃ concentrations, on the excitation intensities,

TABLE 1 Results of bi-exponential fits of the luminescence decay curves of each circular polarization for both solution and solid Eu(facam)₃, including the relative differences between τ_L and τ_R , and the weighted average decay times (τ_{avg})

Eu (facam)₃, DMSO					
	A₁	τ₁	A₂	τ₂	τ_{avg}
L-CPL	0.48	179	0.52	375	281 ± 4
R-CPL	0.81	216	0.19	407	252 ± 2
g_{lf}	-	-0.19	-	-8×10^{-2}	+0.11
Eu (facam)₃, solid					
	A₁	τ₁	A₂	τ₂	τ_{avg}
L-CPL	0.11	110	0.89	435	393 ± 7
R-CPL	0.14	191	0.86	481	439 ± 3
g_{lf}	-	-0.54	-	-0.10	-0.11

or on the excitation wavelength (see Figure S2). Taking the amplitude-weighted average lifetime, $\tau_{\text{avg}} = (A_1\tau_1 + A_2\tau_2)/(A_1 + A_2)$ from the bi-exponential fits,¹⁹ we obtained $g_{\text{lif}} \sim 0.11$, an order of magnitude larger than the uncertainty in this value.

It should be noted that we found no difference in decay rates between the two circular polarizations at the other Eu(facam)₃ emission lines. This could be due to the uniquely large g_{lum} at 595 nm. Smaller differences in lifetimes would fall below our $g_{\text{lif}} \sim 0.01$ detection threshold. It is also possible that only the 595-nm line displays this difference, but this is most likely not the case. In Figure 3e, we measured a second emission line of the Eu(facam)₃ complex, at 614 nm, which is characterized by a g_{lum} , an order of magnitude lower (+0.078). Indeed, the normalized logarithmic decay curves of the two emitted circular polarizations seem to have the same slopes, and bi-exponential fits to these curves yielded a g_{lif} of 6×10^{-3} , which is basically zero within our accuracy.

As discussed earlier, the appearance of a difference in the decay rates between the two circular polarizations implies that the Eu(facam)₃ dissolved in DMSO is a heterogeneous sample. This conclusion is strengthened by the fact that the emission decay curves of the two circular polarizations fitted well bi-exponential (or higher multi-exponential) functions (see) and fitting parameters in Table 1. This is most likely indicative of at least two populations of emitters in the sample, each having a different g_{lum} and emission lifetime. This can be illustrated in the following way, assuming two different populations of complexes in the solution: Now we assume the two excited-state populations to be $N(t), N'(t)$ with emission rates:

$$A = A_L + A_R + A_{\text{NR}}, A' = A'_L + A'_R + A'_{\text{NR}}$$

Then the total time-dependent emission intensity would be

$$I(t) = (A_L + A_R + A_{\text{NR}})N(t) + (A'_L + A'_R + A'_{\text{NR}})N'(t)$$

and the time-dependent circularly polarized emission intensities would be

$$I_L(t) = A_L N(t) + A'_L N'(t) = A_L N_0 e^{-At} + A'_L N'_0 e^{-A't}$$

$$I_R(t) = A_R N(t) + A'_R N'(t) = A_R N_0 e^{-At} + A'_R N'_0 e^{-A't}$$

It seems that unlike the robust eight-dentate CsEu(hfbc)₄ complex, the six-dentate Eu(facam)₃ has more freedom to either move out of the symmetric C₃

conformation or produce a fluctuating structure. It could also incorporate solvent molecule(s) in the ligand shell, thereby producing multiple conformations in the solution, with possible slow interconversion between them, but longer than the emission lifetime scale.

In order to understand the role of the solvent in the configurational heterogeneity of $\text{Eu}(\text{facam})_3$, we investigated the effects of water on its TR-CPL, because, as already mentioned, water is known to slightly affect its ECID. We measured an anhydrous sample dissolved in DMSO, then added 0.5% v/v H_2O , and measured again after several hours (Figure 4).

As can be seen in Figure 4a, the addition of H_2O causes a small decrease in the observed lifetime due to the quenching by the OH vibrational overtones,^{20,21} which increases the non-radiative decay rate. This is verified by the concurrent decrease in luminescence intensity (inset of Figure 4a). Moreover, a nontrivial effect of H_2O contamination is the change in decay profile, from a multi-exponential to nearly single exponential. This occurs in parallel to the disappearance of the decay lifetime difference between the two circular polarizations, which is substantial in the anhydrous sample. This is also evident in Figure 4b where the $g_{lum}(t)$ of the H_2O -contaminated sample is virtually constant throughout the decay. Quantitatively, g_{lif} of the H_2O -contaminated solution is decreased to $\sim 1 \times 10^{-2}$, right at the uncertainty level, and an order of magnitude smaller than the anhydrous DMSO sample.

We believe that these two occurrences, the disappearance of the difference in lifetimes between the two polarizations and the change to a single exponential decay, are due to the sample becoming homogeneous in the presence of H_2O . Because $\text{Eu}(\text{facam})_3$ is under-coordinated, we hypothesize that a water molecule (or two) binds to the Eu^{3+} ion in the first coordination sphere for all $\text{Eu}(\text{facam})_3$ in solution, stabilizing a single species of the complex. It is well known that $\text{Eu}(\text{facam})_3$ can coordinate OH bearing molecules, as it was commonly used as a chiral NMR shift reagent for alcohols (see, e.g., ref. 22).

We have also measured a dried solid sample of $\text{Eu}(\text{facam})_3$ (see Figures S3 and S4). The sample was dissolved in DMSO, drop-cast from solution on a glass substrate, and revealed luminescence and ECID lineshape almost identical to the solution phase. Here also, a difference between the decay rates of the two circular polarizations was found. A bi-exponential function again fitted well the two curves, and similar to the solvated $\text{Eu}(\text{facam})_3$, there were ~ 200 - and $\sim 400\text{-}\mu\text{s}$ lifetime components (see Table 1). However, the weight of the longer lifetime component was much larger, yielding longer weighted average lifetimes for the solid case. Interestingly, $g_{lif} \sim -0.11$ was obtained, which is the same magnitude as in the solution case albeit with an opposite sign

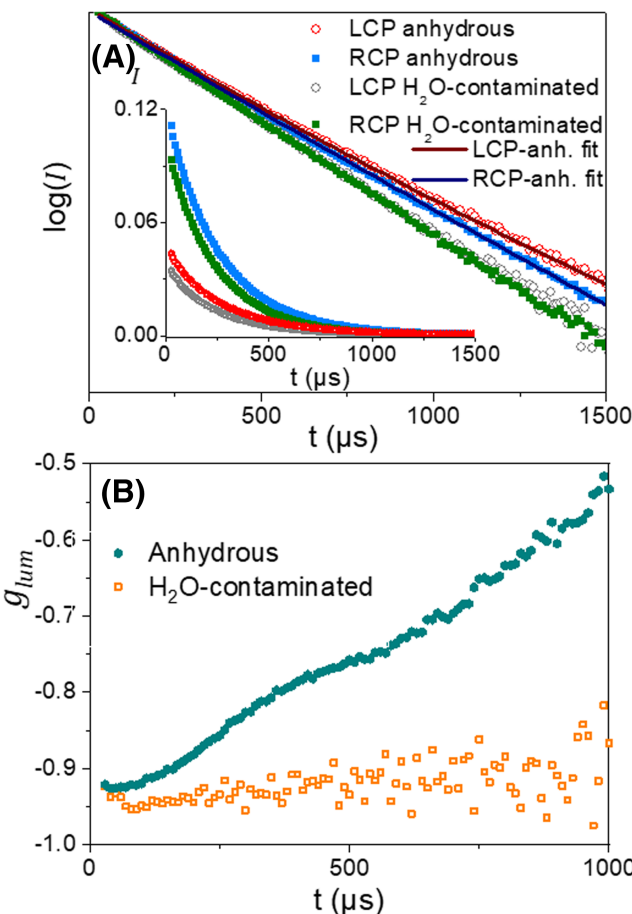


FIGURE 4 The effect of trace amounts of H_2O on the TR-CPL of 12.5-mM $\text{Eu}(\text{facam})_3$ dissolved in DMSO. Excitation wavelength = 405 nm at 40 mW. The data are an average of 100,000 measurement cycles per each emitted circular polarization for the H_2O -contaminated case and 6000 cycles for the anhydrous case. (a) The normalized logarithm of the intensities of the two emitted circular polarizations (at 595 nm) for the anhydrous case and the H_2O -contaminated case. The H_2O -contaminated decay curves were fitted with a single exponent, and the lifetimes were 239 ± 4 and $237 \pm 2 \mu\text{s}$ for the L- and R-CPL decays, respectively. Inset of (a) is the raw intensity decay of the two circular polarization for both cases plotted on a linear scale. (b) The time-dependent dissymmetry factor, $g_{lum}(t)$, measured at 595 nm, for the anhydrous case and the H_2O -contaminated case

(for a detailed explanation, see Figure S4). The solid heterogeneity could be due to different crystalline phases containing occasional DMSO and/or water molecules in the lattice, forming different environments for the Eu^{3+} ions, or having part of the complex crystallized, whereas another part remains amorphous. In any case, the heterogeneity of the solid $\text{Eu}(\text{facam})_3$ is probably static, whereas in the solution, it is more likely to be dynamic.

A radically different Eu^{3+} compound was also examined: an aqueous colloidal dispersion of chiral Eu^{3+} -doped $\text{TbPO}_4\text{-D}_2\text{O}$ lanthanide NCs, which crystallize in

the chiral P3₁21 (or P3₂1) space group.^{23,24} The two NC enantiomers, labeled “D-NC” and “L-NC,” were synthesized as described in ref.¹¹, where L- or D-tartaric acid were used to direct the handedness of the formed NCs. NCs similar to those synthesized in ref.¹¹ were obtained, as evident by transmission electron microscopy imaging (see Figure S5).

Here, we used 488-nm excitation to excite the Tb³⁺ $^7F_6 \rightarrow ^5D_4$ transition. The Tb³⁺ ions transfer the excitation to the dopant Eu³⁺ ions, which subsequently emit at various $^5D_0 \rightarrow ^7F_J$ ($J = 0-6$) transitions.²⁵ Inter Tb³⁺-Tb³⁺, Eu³⁺-Eu³⁺ energy transfer within individual NCs and Eu³⁺-Tb³⁺ back-transfer may also occur, resulting in a complex energy migration network in the

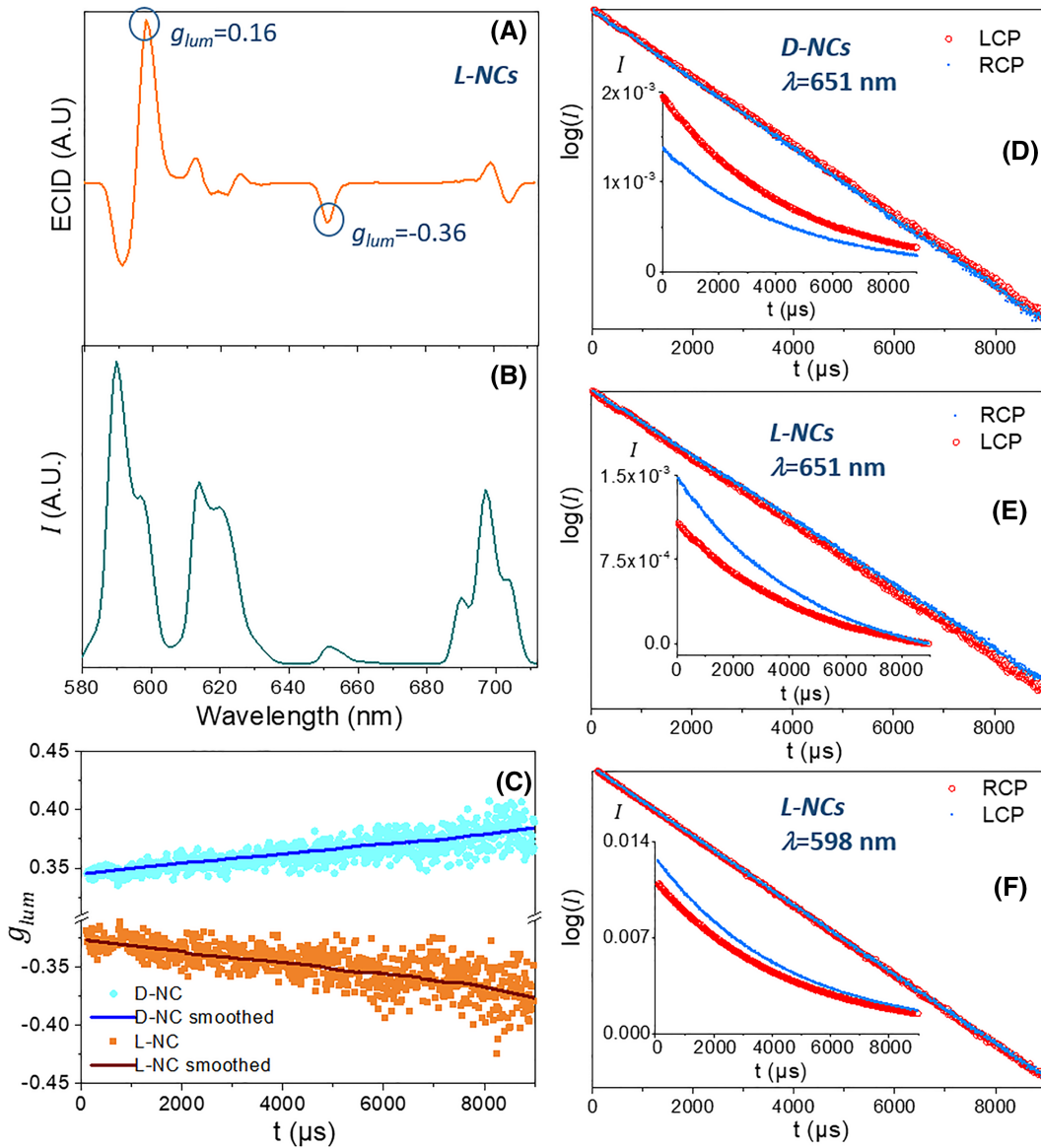


FIGURE 5 The total luminescence, ECID, and emission decay curves at 650 nm of R- and L-CPL of excitation wavelength = 488 nm with 60-mW power. The data are an average of 370,000 repetitions per each emitted circular polarization. (a) ECID and (b) total emission spectra of colloidal solution of D- and L-Eu³⁺-doped TbPO₄·D₂O NCs. (c) The time-dependent dissymmetry factor, $g_{lum}(t)$, plotted for the D- and L-NCs, again showing the opposite behavior of the two enantiomers. The semitransparent dots are the measured values, and the lines are smoothed guides to eye. (d) The normalized logarithms of the emission intensities for the two circular polarizations in the D-NC sample are plotted. The curves were fitted with a single exponent, and the lifetimes were 4602 ± 20 and 4713 ± 11 μs for the L- and R-CPL decays, respectively. (e) The same as (d) but for the L-NCs. The inversion of the trend in lifetime magnitudes of the L- and R-CPL curves with respect to the D-NCs can be observed. The curves were fitted with a single exponent and the lifetimes were 4516 ± 18 and 4447 ± 15 μs for the L- and R-CPL decays, respectively. (f) A control sample; a measurement of the 598-nm line with a lower g_{lum} ($g_{lum} = 0.16$) showing no difference in the decay rates of the L- and R-CPL emission curves. Insets of (d), (e), and (f) are the raw emission intensity decays of the two circular polarizations plotted on a linear scale

NCs over relatively long timescales ($\sim 10^{-3}$ s). The highest g_{lum} value for the $^5D_0 \rightarrow ^7F_1$ transition in this system is only 0.15, much lower with respect to Eu(facam)₃; hence, we could not measure a significant difference between the lifetimes of the two circular polarizations for this transition in the NCs (see Figure 5f). We therefore focused on the NC emission line with the highest dissymmetry factor, the $^5D_0 \rightarrow ^7F_3$ transition at 650 nm, with $g_{lum} = -0.36$.¹¹ Furthermore, as this is an electric dipole and magnetic dipole forbidden transition, arising due to some J-state mixing, it is the weakest line of the emission line series.^{14,25,26} Hence, measurement of the TR-CPL at this line suffers from low signal-to-noise ratio relative to the Eu(facam)₃ measurements.

Figure 5d,e shows the normalized logarithmic luminescence intensity decay curves of the two circular polarizations for the two NC enantiomers, respectively, and Figure 5c shows the change in $g_{lum}(t)$ as a function of time for the two NC enantiomers. As in the two Eu(facam)₃ cases, $g_{lum}(t)$ starts from the steady-state measurement value of for this line (0.36). The logarithmic decay curves shown in Figure 5d,e can be fitted well with a single exponent with visible different slopes for the two circular polarizations, which invert between the two NC enantiomers. In spite of the good fit to a single exponential function, the observed lifetime difference implies that the Eu³⁺ sites in the NCs are heterogeneous. This could be the result of a sum of multiple decaying exponents with broad lifetime distribution. Here, a value of $g_{lf} = 1.5-2 \times 10^{-2}$ was obtained. Although this value is only a factor of ~ 2 larger than the level of uncertainty in determining the g_{lf} magnitude, the opposite and roughly equal $g_{lum}(t)$ trends observed for the two NC enantiomers, together with the following negative control experiments, prove that the measured lifetime differences for the two enantiomers are real: (i) A racemic mixture of the chiral NCs did not exhibit measurable lifetime differences (see Figure S6). (ii) Measurements of decay curves at a different emission wavelength (598 nm) with lower g_{lum} (0.16) also did not exhibit lifetime differences (see Figure 5f). In the above cases, the normalized logarithmic decay curves of the two emitted circular polarizations seemed to have the same slopes, and single exponential fits to these curves yielded for the racemic NC case $g_{lf} = -5 \times 10^{-3}$ and for 598 nm case $g_{lf} = 6 \times 10^{-3}$, which are around the same as the uncertainty level.

Because TbPO₄ is a rigid crystal, highly insoluble in water (or D₂O), the heterogeneity in this case is almost certainly not due to a dynamic equilibrium in the solution. More likely, this heterogeneity might be due to different types of crystal defects, and different local stoichiometric ratios of D₂O:Eu³⁺ in the unit cells.

Interestingly, Mesbah et al. recently demonstrated the existence of several hydrous phases of such crystals.²⁷

4 | CONCLUSION

We employed TR-CPL measurements to study the emission dynamics and heterogeneity of Eu³⁺-containing systems that exhibit a high degree of chiroptical activity. The difference between the two circularly polarized decay rates was quantified by defining a lifetime dissymmetry factor g_{lf} , similarly to the chiroptical analogs in steady-state CD and ECID spectroscopies for absorption and emission, respectively. It was established that the detection of a difference in lifetimes between the two circular polarizations necessitates a heterogeneous system, which could be either static or dynamic. Therefore, at emissions lines with high g_{lum} , TR-CPL can be a useful tool to establish heterogeneity, in particular in cases where commonly used techniques are insufficient. For example, NMR lines broaden in the regime of intermediate ligand exchange rates, thus preventing determination of heterogeneity; and in the fast exchange regime, although the lines are narrower, the distinction between different species is difficult.¹⁷ In addition, as shown in the case of emitting chiral NCs, TR-CPL was more sensitive than attempted distinction between single and multi-exponential decay.

Lastly, by simply measuring TR-CPL and experimenting with different solvents, we probed the heterogeneity in the common ECID standard Eu(facam)₃ and demonstrated a facile method to achieve a single species.

It is difficult to estimate the lower g_{lum} limit for which it would be possible to measure TR-CPL, as the magnitude of g_{lf} is also dependent on the level of heterogeneity of the system under study. As a general guideline, we would expect that a minimal g_{lum} value on the order of 0.1 would be required for such measurements.

ACKNOWLEDGMENTS

This research was supported by the Israel Science Foundation grant no. 338/18.

DATA AVAILABILITY STATEMENT

Data that support the findings of this study are available in the Supporting Information of this article or are available from the corresponding author upon reasonable request.

ORCID

Francesco Zinna  <https://orcid.org/0000-0002-6331-6219>

Lorenzo Di Bari  <https://orcid.org/0000-0003-2347-2150>

Gil Markovich  <https://orcid.org/0000-0002-4047-189X>

REFERENCES AND NOTES

- Richardson FS, Riehl JP. Circularly polarized luminescence spectroscopy. *Chem Rev.* 1977;77(6):773-792.
- Kumar J, Nakashima T, Kawai T. Circularly polarized luminescence in chiral molecules and supramolecular assemblies. *J Phys Chem Lett.* 2015;6(17):3445-3452.
- Sánchez-Carnerero EM, Agarrabeitia AR, Moreno F, et al. Circularly polarized luminescence from simple organic molecules. *Chem a Eur J.* 2015;21(39):13488-13500.
- Arrico L, Di Bari L, Zinna F. Quantifying the overall efficiency of circularly polarized emitters. *Chem a Eur J.* 2020. <https://doi.org/10.1002/chem.202002791>
- Schauerte JA, Steel DG, Gafni A. Time-resolved circularly polarized protein phosphorescence. *Proc Natl Acad Sci U S a.* 1992;89(21):10154-10158.
- Metcalf DH, Snyder SW, Wu S, et al. Excited-state chiral discrimination observed by time-resolved circularly polarized luminescence measurements. *J Am Chem Soc.* 1989;111(8):3082-3083.
- Meskens SCJ, Dekkers HPJM. Enantioselective quenching of luminescence: molecular recognition of chiral lanthanide complexes by biomolecules in solution. *J Phys Chem a.* 2001;105(19):4589-4599.
- Metcalf DH, Demas JN, Richardson FS, Snyder SW. Chiral discrimination in electronic energy-transfer processes between dissymmetric metal complexes in solution. Time-resolved chiroptical luminescence measurements of enantioselective excited-state quenching kinetics. *J Am Chem Soc.* 1990;112(15):5681-5695.
- MacKenzie LC, Pålsson LO, Parker D, Beeby A, Pal R. Rapid time-resolved circular polarization luminescence (CPL) emission spectroscopy. *Nat Commun.* 2020;11(1):1676.
- Zinna F, Giovanella U, Di Bari L. Highly circularly polarized electroluminescence from a chiral europium complex. *Adv Mater.* 2015;27(10):1791-1795.
- Vinegrad E, Hananel U, Markovich G, Cheshnovsky O. Determination of handedness in a single chiral nanocrystal via circularly polarized luminescence. *ACS Nano.* 2019;13(1):601-608.
- Zinna F, Di Bari L. Lanthanide circularly polarized luminescence: bases and applications. *Chirality.* 2015;27(1):1-13.
- Di Pietro S, Di Bari L. The structure of MLn (hfbc) 4 and a key to high circularly polarized luminescence. *Inorg Chem.* 2012;51(21):12007-12014.
- Koen B. Interpretation of europium (III) spectra. *Coord Chem Rev.* 2015;205:1-46.
- Berova N, Polavarapu PL, Nakanishi K, Woody RW. *Comprehensive Chiroptical Spectroscopy Vol 1.* New-Jersey: Wiley & sons; 2012:791.
- Schippers PH, Buekel AVD, Dekkers HPJM. An accurate digital instrument for the measurement of circular polarisation of luminescence. *J Phys E.* 1982;15(9):945-950.
- Di Bari L, Salvadori P. Solution structure of chiral lanthanide complexes. *Coord Chem Rev.* 2005;249(24):2854-2879.
- Colvin RV, Arajs S, Peck JM. Paramagnetic behavior of metallic cerium and europium. *Phys Rev Lett.* 1961;122:14-18.
- Sillen A, Engelborghs Y. The correct use of 'average' fluorescence parameters. *Photochem Photobiol.* 1998;67:475-486.
- Haas Y, Stein G. Pathways of radiative and radiationless transitions in europium (III) solutions: role of solvents and anions. *J Phys Chem.* 1971;75(24):3668-3677.
- Voloshin AI, Shavaleev NM, Kazakov PV. Water enhances quantum yield and lifetime of luminescence of europium (III) tris-β-diketonates in concentrated toluene and acetonitrile solutions. *JOL.* 2001;93(3):191-197.
- Ghosh I, Zeng H, Kishi Y. Application of chiral lanthanide shift reagents for assignment of absolute configuration of alcohols. *Org Lett.* 2004;6(25):4715-4718.
- Di W, Li J, Shirahata N, Sakka Y, Willinger MG, Pinna N. Photoluminescence, cytotoxicity and in vitro imaging of hexagonal terbium phosphate nanoparticles doped with europium. *Nanoscale.* 2011;3(3):1263-1269.
- Fang YP, Xu AW, Song RQ, et al. Systematic synthesis and characterization of single-crystal lanthanide orthophosphate nanowires. *J Am Chem Soc.* 2003;125(51):16025-16034.
- Holloway WW, Kestigian M, Newman R. Direct evidence for energy transfer between rare earth ions in terbium-europium tungstates. *Phys Rev Lett.* 1963;11(10):458-460.
- Carr R, Evans NH, Parker D. Lanthanide complexes as chiral probes exploiting circularly polarized luminescence. *Chem Soc Rev.* 2012;41(23):7673-7686.
- Mesbah A, Clavier N, Elkaim E, Szenknect S, Dacheux N. In pursuit of the rhabdophane crystal structure: from the hydrated monoclinic LnPO₄·0.667H₂O to the hexagonal LnPO₄ (Ln = Nd, Sm, Gd, Eu and Dy). *J Solid State Chem.* 2017;249:221-227.

SUPPORTING INFORMATION

Additional supporting information may be found online in the Supporting Information section at the end of this article.

How to cite this article: Hananel U, Schwartz G, Paiss G, et al. Time-resolved circularly polarized luminescence of Eu³⁺-based systems. *Chirality.* 2021;33:124-133. <https://doi.org/10.1002/chir.23293>